

# Predictive Modeling in the Reservoir Kernel Motif Space

Peter Tiño

School of Computer Science  
University of Birmingham  
Birmingham, UK  
p.tino@bham.ac.uk

Robert Simon Fong

Theory Lab, Central Research Institute  
2012 Labs, Huawei Technologies Co. Ltd.  
Hong Kong SAR, China.  
fong.robert.simon1@huawei.com

Roberto Fabio Leonarduzzi

Theory Lab, Central Research Institute  
2012 Labs, Huawei Technologies Co. Ltd.  
Hong Kong SAR, China.  
leonarduzzi.roberto.fabio@huawei.com

**Abstract**—This work proposes a time series prediction method based on the kernel view of linear reservoirs. In particular, the time series motifs of the reservoir kernel are used as representational basis on which general readouts are constructed. We provide a geometric interpretation of our approach shedding light on how our approach is related to the core reservoir models and in what way the two approaches differ. Empirical experiments then compare predictive performances of our suggested model with those of recent state-of-art transformer based models, as well as the established recurrent network model - LSTM. The experiments are performed on both univariate and multivariate time series and with a variety of prediction horizons. Rather surprisingly we show that even when linear readout is employed, our method has the capacity to outperform transformer models on univariate time series and attain competitive results on multivariate benchmark datasets. We conclude that simple models with easily controllable capacity but capturing enough memory and subsequence structure can outperform potentially over-complicated deep learning models. This does not mean that reservoir motif based models are preferable to other more complex alternatives - rather, when introducing a new complex time series model one should employ as a sanity check simple, but potentially powerful alternatives/baselines such as reservoir models or the models introduced here.

**Index Terms**—Reservoir Computing, Time Series Forecasting, Kernel Methods, Recurrent Neural Network

## I. INTRODUCTION

Time series forecasting methods emerge within two main paradigms. The first paradigm essentially “trades time for space/memory,” treating the historical time series as a static input to the model, which is then processed spatially.

Recent successful examples of this paradigm include transformer architectures [1]. Since their inception, transformers have exhibited exceptional performance in various tasks, including natural language processing (NLP) [2]. Recently, transformers have also been applied to time-series forecasting tasks, as demonstrated in [3], [4]. However, as [5] pointed out, whilst multi-head self-attention captures semantic correlations amongst elements of a time series, the temporal correlation is disregarded due to the nature of the static input.

The second paradigm captures temporal dependencies in the input data stream through a parametric state-space modelling. Time series data are sequentially encoded into this state space, allowing dynamic capture of temporal information via state-

space vectors. Notable examples of this approach include Recurrent Neural Networks and Kalman filters [6].

In this work we consider a special class of Recurrent Neural Networks known as Reservoir Computing models [7]–[10], where the state space representation and update is fixed and non-trainable. In particular, Echo State Network (ESN) [7], [11]–[13] is one of the simplest representations of the Reservoir Computing paradigm, which comprises of a recurrent neural network with a fixed driven dynamical system (reservoir), a fixed input-to-state space mapping, and a simple trainable linear readout map from state space to output.

The term “Reservoir Computing” is derived from the concept that the reservoir states provide an “echo” of the entire input history, independent of the initial state (Echo State Property). To that end, the reservoir weights are typically rescaled such that the largest singular value of the state coupling weight matrix is less than 1.

Echo State Networks (ESNs) have been successfully applied in a diverse range of tasks [13]–[15]. Numerous extensions to the classical ESN model have been proposed, including deep ESNs [16], intrinsic plasticity [17], [18], decoupled reservoirs [19], leaky-integrator reservoir units [20], and filter neurons with delay-and-sum readout [21], among others. Furthermore, a similar state-space model approach has been recently rediscovered in [22] and its associated work.

Recently, a kernel perspective on linear ESNs was provided in [23], wherein the state-space representation of (potentially left infinite) input time series is viewed as the feature map corresponding to the reservoir kernel. Due to the linear nature of the reservoir, the canonical dot product of such feature representations of two input time series can be written analytically as an inner product of the time series themselves. The metric tensor corresponding to this inner product can be used to reveal the representational structure applied by the given reservoir model to the driving input time series. In particular, the eigenvectors and the associated eigenvalues of the metric tensor correspond to the dominant projection axes (time series ‘motifs’) along with their scaling (‘importance’) factors, respectively.

We propose to use the reservoir time series motifs as the representational basis on which general readouts can be built. Unlike in the original reservoir model that pre-assigns

eigenvalues to motifs, we allow for learnable feature scaling. Surprisingly, this simple reservoir motif based architecture outperforms transformers on a number of univariate benchmark problems and achieves comparable performance in a variety of multi-variate benchmark problems.

After a brief summary of the kernel view of ESNs in Section II, we provide a geometric view of our approach in Section IV, where we explain in detail how our approach is related to the core reservoir models and in what way the two approaches differ. Experiments in section V compare predictive performances of our suggested model with those of recent state-of-art transformer based models, as well as the established recurrent network model - LSTM. The predictive modelling experiments are performed on both univariate and multivariate time series and with a variety of prediction horizons. Finally, Section VI summarizes and discusses the main results of this study.

## II. LINEAR RESERVOIR AS A TEMPORAL KERNEL

This section briefly summarizes the kernel view of linear reservoir systems presented in [23]. Consider a linear reservoir system  $R := (\mathbf{W}, \mathbf{w}, h)$  operating on univariate input, where  $\mathbf{W} \in \mathbb{R}^{N \times N}$  and  $\mathbf{w} \in \mathbb{R}^N$  are the dynamic and input couplings, respectively, and  $h : \mathbb{R}^N \rightarrow \mathbb{R}^d$  is a trainable readout map. The corresponding driven linear dynamical system is given by:

$$\begin{cases} \mathbf{x}(t) = \mathbf{W}\mathbf{x}(t-1) + u(t)\mathbf{w} \\ \mathbf{y}(t) = h(\mathbf{x}(t)), \end{cases} \quad (\text{II.1})$$

where  $\{u(t)\}_t \subset \mathbb{R}$ ,  $\{\mathbf{x}(t)\}_t \subset \mathbb{R}^N$ , and  $\{\mathbf{y}(t)\}_t \subset \mathbb{R}^d$  denote the inputs, states and outputs, respectively.

Given two sufficiently long time series of length  $\tau > N$ ,

$$\begin{aligned} \mathbf{u} &= (u(-\tau+1), u(-\tau+2), \dots, u(-1), u(0)) \\ &=: (u_1, u_2, \dots, u_\tau) \in \mathbb{R}^\tau \end{aligned}$$

and

$$\begin{aligned} \mathbf{v} &= (v(-\tau+1), v(-\tau+2), \dots, v(-1), v(0)) \\ &=: (v_1, v_2, \dots, v_\tau) \in \mathbb{R}^\tau \end{aligned}$$

we consider the reservoir states reached upon reading them (with zero initial state) their feature space representations [23]:

$$\phi(\mathbf{u}) = \sum_{j=1}^{\tau} u_j \mathbf{W}^{\tau-j} \mathbf{w}, \quad \phi(\mathbf{v}) = \sum_{j=1}^{\tau} v_j \mathbf{W}^{\tau-j} \mathbf{w}.$$

The canonical dot product (reservoir kernel)

$$K(\mathbf{u}, \mathbf{v}) = \langle \phi(\mathbf{u}), \phi(\mathbf{v}) \rangle$$

can be written in the original time series space as a semi-inner product  $\langle \mathbf{u}, \mathbf{v} \rangle_Q = \mathbf{u}^\top \mathbf{Q} \mathbf{v}$ , where

$$Q_{i,j} = \mathbf{w}^\top (\mathbf{W}^\top)^{i-1} \mathbf{W}^{j-1} \mathbf{w}.$$

Since the (semi-)metric tensor  $\mathbf{Q}$  is symmetric and positive semi-definite, it admits the following eigen-decomposition:

$$\mathbf{Q} = \mathbf{M} \Lambda_Q \mathbf{M}^\top, \quad (\text{II.2})$$

where  $\Lambda_Q := \text{diag}(\lambda_1, \lambda_2, \dots, \lambda_{N_m})$  is a diagonal matrix consisting of non-negative eigenvalues of  $\mathbf{Q}$  with the corresponding eigenvectors  $\mathbf{m}_1, \mathbf{m}_2, \dots, \mathbf{m}_{N_m} \in \mathbb{R}^\tau$  (columns of  $\mathbf{M}$ ). The  $N_m := \text{rank}(\mathbf{Q}) \leq N \leq \tau$  eigenvectors of  $\mathbf{M}$  with positive eigenvalues are called the *motifs* of  $R$ . We have:

$$K(\mathbf{u}, \mathbf{v}) = \left( \Lambda_Q^{\frac{1}{2}} \mathbf{M}^\top \mathbf{u} \right)^\top \left( \Lambda_Q^{\frac{1}{2}} \mathbf{M}^\top \mathbf{v} \right).$$

In particular, the reservoir kernel is a canonical dot product of time series projected onto the motif space spanned by  $\{\mathbf{m}_i\}_{i=1}^{N_m}$ :

$$K(\mathbf{u}, \mathbf{v}) = \langle \tilde{\mathbf{u}}, \tilde{\mathbf{v}} \rangle,$$

where

$$\tilde{\mathbf{u}} = \Lambda_Q^{\frac{1}{2}} \mathbf{M}^\top \mathbf{u} \quad (\text{II.3})$$

$$= \begin{bmatrix} \lambda_1^{\frac{1}{2}} \cdot \langle \mathbf{m}_1, \mathbf{u} \rangle \\ \vdots \\ \lambda_{N_m}^{\frac{1}{2}} \cdot \langle \mathbf{m}_{N_m}, \mathbf{u} \rangle \end{bmatrix} \quad (\text{II.4})$$

$$= \left( \lambda_i^{\frac{1}{2}} \cdot \langle \mathbf{m}_i, \mathbf{u} \rangle \right)_{i=1}^{N_m} \in \mathbb{R}^{N_m}. \quad (\text{II.5})$$

## III. PREDICTIVE MODEL BASED ON RESERVOIR MOTIFS

In this Section we propose a simple predictive model motivated by the kernel view of Reservoir Computing. In the view of motif space representations  $\tilde{\mathbf{u}}$  of time series  $\mathbf{u}$  of length  $\tau$  ( $\tau$ -blocks), we propose to also represent the observed  $\tau$ -blocks of input time series in the reservoir motif space  $\text{span}(\{\mathbf{m}_i\}_{i=1}^{N_m})$ , but instead of using the associated mixing weights  $\lambda_i^{\frac{1}{2}}$  imposed by the reservoir, we allow the *motif coefficients*,  $C := \{c_i \in \mathbb{R}\}_{i=1}^{N_m}$  to be adaptable:

$$\varphi(\mathbf{u}; C) = \begin{bmatrix} c_1 \cdot \langle \mathbf{m}_1, \mathbf{u} \rangle \\ \vdots \\ c_{N_m} \cdot \langle \mathbf{m}_{N_m}, \mathbf{u} \rangle \end{bmatrix} \quad (\text{III.1})$$

$$= (c_i \cdot \langle \mathbf{m}_i, \mathbf{u} \rangle)_{i=1}^{N_m} \in \mathbb{R}^{N_m}. \quad (\text{III.2})$$

For a real sequence  $\mathbf{z} = \{z(t)\}_{t \in \mathbb{Z}}$ , denote by  $\mathbf{z}(t, \tau) \in \mathbb{R}^\tau$  the  $\tau$ -block of consecutive elements of  $\mathbf{z}$  ending with  $z(t)$ , i.e.

$$\mathbf{z}(t, \tau) = (z(t-\tau+1), \dots, z(t-2), z(t-1), z(t)).$$

The  $\tau$ -block  $\mathbf{z}(t, \tau)$  will be represented through

$$\varphi(\mathbf{z}(t, \tau); C) := (c_i \cdot \langle \mathbf{m}_i, \mathbf{z}(t, \tau) \rangle)_{i=1}^{N_m} \in \mathbb{R}^{N_m},$$

and based on this representation the associated output will be calculated through a readout map  $q : \mathbb{R}^{N_m} \rightarrow \mathbb{R}^d$ ,

$$\mathbf{y}(t) = q(\varphi(\mathbf{z}(t, \tau); C)).$$

Note that the scaling coefficients  $C$  can be actually included in the readout map, so no separate motif weights need to be learnt. Indeed, consider a readout map with unit motif weights  $\tilde{q} : \mathbb{R}^{N_m} \rightarrow \mathbb{R}^d$  defined by:

$$\tilde{q}(x_1, \dots, x_{N_m}) := q(c_1 \cdot x_1, \dots, c_{N_m} \cdot x_{N_m}).$$

Then

$$\tilde{q}\left(\left(\langle \mathbf{m}_i, \mathbf{u}(t, \tau) \rangle\right)_{i=1}^{N_m}\right) = q\left(\left(c_i \cdot \langle \mathbf{m}_i, \mathbf{z}(t, \tau) \rangle\right)_{i=1}^{N_m}\right).$$

We will thus build predictive models reading out the responses from the recent  $\tau$ -block histories  $\mathbf{z}(t, \tau)$  of input time series  $\mathbf{z}$  based on orthogonal projections of those histories onto the reservoir motif space (note that the motifs  $\{\mathbf{m}_i\}_{i=1}^{N_m}$  constitute an orthonormal set of axis vectors):

$$\begin{aligned} \mathbf{y}(t) &= q(\varphi(\mathbf{z}(t, \tau); \mathbb{1})) \\ &= q(\mathbf{M}^\top \mathbf{z}(t, \tau)). \end{aligned}$$

We refer to our model as the *Reservoir Motif Machine* (RMM). Whilst the notion of RMM is inspired by Reservoir Computing, it does not belong to the Reservoir Computing paradigm, as illustrated by the next section.

#### IV. GEOMETRIC VIEW

Given a time series and a sufficiently long  $\tau$ -block  $\mathbf{u} \in \mathbb{R}^\tau$  of recently observed items, the reservoir state reached after reading the time series can be approximated by

$$\phi(\mathbf{u}) = \sum_{j=1}^{\tau} u_j \mathbf{W}^{\tau-j} \mathbf{w} = \mathbf{A} \mathbf{u},$$

where  $\mathbf{A} \in \mathbb{R}^{N \times \tau}$  is a linear operator (matrix) with columns  $\{\mathbf{W}^{\tau-j} \mathbf{w}\}_{j=1}^{\tau}$ .

The operator  $\mathbf{A}$  projects the time series  $\mathbf{u}$  onto  $\mathbb{R}^{N_m}$ . Consider the SVD-decomposition of  $\mathbf{A}$  given by the eigen-decomposition of

$$\mathbf{A}^\top \mathbf{A} = \mathbf{V} \mathbf{D} \mathbf{V}^\top,$$

where

$$\mathbf{V} = [\mathbf{v}_1, \mathbf{v}_2, \dots, \mathbf{v}_\tau]$$

is a matrix that stores the eigenvectors of  $\mathbf{A}^\top \mathbf{A}$  as columns and  $\mathbf{D} = \text{diag}(d_1, d_2, \dots, d_\tau)$  is a diagonal matrix of the corresponding eigenvalues  $d_1 \geq d_2 \geq \dots \geq d_\tau$ . Since  $d_{N+1} = d_{N+2} = \dots = d_\tau = 0$ , geometrically, the operator  $\mathbf{A}$  maps the unit  $\tau$ -sphere

$$S = \{\mathbf{x} \in \mathbb{R}^\tau \mid \|\mathbf{x}\| = 1\}$$

onto an ellipsoid with semi-axis of length  $d_1^{\frac{1}{2}}, d_2^{\frac{1}{2}}, \dots, d_N^{\frac{1}{2}}$  oriented along  $\mathbf{v}_1, \mathbf{v}_2, \dots, \mathbf{v}_N \in \mathbb{R}^\tau$ .

We now realize that  $\mathbf{Q} = \mathbf{A}^\top \mathbf{A}$  and hence the ellipsoid's semi-axis are equal to the reservoir motifs. The reservoir dynamics maps the unit sphere  $S$  of possibly long  $\tau$ -blocks (normalized to norm 1) onto an ellipsoid with semi-axis of length  $\lambda_1^{\frac{1}{2}}, \lambda_2^{\frac{1}{2}}, \dots, \lambda_{N_m}^{\frac{1}{2}}$  oriented along the reservoir motifs  $\mathbf{m}_1, \mathbf{m}_2, \dots, \mathbf{m}_{N_m} \in \mathbb{R}^\tau$ . In other words, long histories of input time series are represented through low dimensional representations given projections onto the  $N_m \leq N < \tau$  dimensional subspace formed the reservoir motif basis.

We emphasize that our time series representations

$$\varphi(\mathbf{z}(t, \tau); \mathbb{1}) = \mathbf{M}^\top \mathbf{z}(t, \tau)$$

are not approximating the reservoir state reached upon reading  $\mathbf{z}$  up to time  $t$ , but are projections of  $\mathbf{z}(t, \tau)$  onto the feature space defined by the reservoir kernel.

In this section we demonstrate the performance of our simple RMM predictive model. To keep the model efficient we constrain ourselves to linear readouts only. We will thus solely employ linear RMMs (Lin-RMM). On a variety of tasks Lin-RMMs are compared with the corresponding reservoir models, as well as with a selection of state-of-the-art methods.

Even though we presented the model development for univariate inputs, the model can be easily extended to the multivariate case e.g., as done here, by representing each of the input univariate channels separately as outlined above and then feeding the joint representation into the linear readout. Other more sophisticated methods based on tensor calculus are possible.

#### A. Datasets

To facilitate the comparison of our results with the state-of-the-art, we have used the same datasets and the same experimental protocols used in the recent time series forecasting papers [3], [4]. Those are briefly described below for the sake of completeness. Dataset details are summarized in Table I.

a) *ETT*: The Electricity Transformer Temperature dataset<sup>1</sup> consists of measurements of oil temperature and six external power-load features from transformers in two regions of China. The data was recorded for two years, and measurements are provided either hourly (indicated by 'h') or every 15 minutes (indicated by 'm'). The ETTh1, ETTh2 and ETTm1 datasets were used for univariate prediction of the oil temperature variable, while the ETTm2 dataset was used for multivariate prediction of all variables.

b) *ECL*: The Electricity Load Diagrams<sup>2</sup> consists of hourly measurements of electricity consumption in kWh for 370 Portuguese clients during four years. The dataset was used for univariate prediction for client MT 320 and multivariate prediction of all clients.

c) *Weather*: The Local Climatological Data (LCD) dataset<sup>3</sup> consists of hourly measurements of climatological observations for 1600 weather stations across the US during four years. The dataset was used for univariate prediction of the Wet Bulb Temperature variable and for multivariate prediction of all variables.

d) *Exchange*: The Exchange dataset [24] consists of the daily exchange rates of the currencies of 8 countries (Australia, Great Britain, Canada, China, Japan, New Zealand, Singapore and Switzerland) from 1990 to 2016. The dataset was used for multivariate prediction of all exchange rates.

e) *ILI*: The Influenza-Like Illness dataset<sup>4</sup> consists of the weekly data on the number of patients with influenza-like symptoms, in different age groups, visiting clinics in the US, between 2002 and 2020. The dataset was used for multivariate prediction of all variables.

<sup>1</sup><https://github.com/zhouhaoyi/ETDataset>

<sup>2</sup><https://archive.ics.uci.edu/dataset/321/electricityloaddiagrams20112014>

<sup>3</sup><https://www.ncei.noaa.gov/data/local-climatological-data/>

<sup>4</sup><https://gis.cdc.gov/grasp/fluview/fluportaldashboard.html>

TABLE I  
DATASET DETAILS. LENGTH, DIMENSION AND SAMPLING PERIOD FOR ALL DATASETS.

Dataset	Length	Dimension	Period
ETTh	17420	7	1 hour
ETTm	69680	7	15 minutes
ECL	26304	321	1 hour
Weather	52696	22	1 hour
Exchange	7588	8	1 day
ILI	966	8	1 week

## B. Experimental setup

The typical choice of sampling random reservoir coupling matrices [7], [10] requires numerous trials and even luck [19], because principled strategies for the construction of appropriate random reservoirs have not been adequately devised. Alternatively, empirical comparisons and theoretical arguments in [23], [25] showed that simple cycle reservoirs, with just two degree of freedom - the input weight  $r_{in} > 0$  and the cycle weight  $0 < \rho < 1$  (which is also spectral radius of the reservoir coupling  $\mathbf{W}$ ) - can achieve comparable or even superior performance to that of random reservoirs. Moreover, [26] showed that such cyclic reservoirs are universal. In consequence, we adopted this architecture and constructed the motifs  $\{\mathbf{m}_i\}$  from Simple Cycle Reservoirs. The input weights all have the same absolute value  $r_{in}$  and an aperiodic sign pattern generated deterministically based on expansion of an irrational number (in our case  $\pi$ ) [25]. We used grid search on the validation splits to select the spectral radius  $\rho \in \{0.9, 0.99, 0.999, 0.9999\}$  and the input weight  $r_{in} \in \{0.01, 0.05, 0.1, 1\}$ . Based on preliminary simulations on the validation sets, we fix  $\tau = 336$  for the look-back window length and reservoir size to  $N = 150 < \tau/2 = 168$ . The historic horizon  $\tau$  is large enough to capture the relevant information for prediction, and further increasing it showed negligible performance gains.

To train the linear readout in the Lin-RMM we used ridge regression with ridge coefficient of  $10^{-4}$ .

We compare prediction errors obtained with our Lin-RMM with those of state-of-the-art transformer models published recently in the literature [3], [4]. To allow for direct comparisons of the results, we copy the experimental setting of [3], [4] in that we use:

- the *same* datasets with the same train/validation/test splits of the data,
- the *same* prediction horizons, and
- the *same* performance measures, namely mean square and mean absolute error, MSE and MAE, respectively.

The results of the alternative models are reproduced directly from [3], [4].

For univariate time series, we compare our results with those of the state-of-the-art Informer, a transformer-based prediction model [3]. The study [3] reports extensive comparisons be-

tween Informer and other models such as ARIMA and LSTM, and found the former to outperform all the others.

For multivariate time series, the more recent FEDformer [4] was shown to outperform Informer, so we use the results reported in [4] as a comparison baseline.

## C. Time series prediction

1) *Univariate prediction*: Table III shows the mean-squared and absolute prediction errors, MSE and MAE, respectively, for univariate time series, compared to the Informer results published in [3], for several prediction horizons. First, it can be seen that Lin-RMM surprisingly outperforms all competitors models in both metrics.

While in principle it may seem surprising that the simple Lin-RMM outperforms models with potentially much larger capacity and expressive power, we conjecture that the explanation lies in the possibility of straightforward inclusion of selective long memory captured in the reservoir motifs and the relatively low amount of data available for training. While linear models based on motif convolutions have, in principle, a larger model bias, they can be learned with a much smaller variance. In consequence, in tasks where the model bias is not too large, the large variance associated with learning complex models from a small dataset dominates. As the prediction horizon increases, the tasks become more difficult and the model bias increases; consequently, the performance gap between the Lin-RMM and Informer decreases. Still, even in these cases the motif convolution features retain their edge. More substantial theoretical analysis is the matter of our future work.

2) *Multivariate prediction*: Table III shows the mean-squared and absolute prediction errors for multivariate time series, compared to the FEDformer model (in its Fourier and Wavelet versions, f-FEDformer and w-FEDformer, respectively) introduced in [4]. It can be seen from Table III that, for the potentially more difficult task of multivariate prediction the performance differences are more balanced: FEDformer offers superior performance in two of the larger datasets (Exchange and Weather), while Lin-RMM dominates in the other two smaller ones (ETTm2, ILI).

## D. Comparisons of RMM with RC

So far we have demonstrated the surprising power of the Lin-RMM model, but how does it fare when compared to the reservoir model (Simple Cycle Reservoir) from which the motif base was constructed? As we argued in section IV the sequence representations in Lin-RMM are not equal to those in the corresponding reservoir model.

We compare Lin-RMM with the corresponding reservoir models (linear dynamics) with both linear (L-RC) and non-linear (NL-RC) readouts (MLP with cross-validated model complexity). For the sake of brevity, we focus only on the results on univariate prediction.

Table IV shows the prediction errors for all the models under consideration. It can be seen that performance of all models is

TABLE II  
UNIVARIATE PREDICTION PERFORMANCE. OUR LIN-RMM MODEL IS COMPARED WITH THE INFORMER, LSTM AND ARIMA MODELS BASED ON THEIR PERFORMANCE RESULTS REPORTED IN [3] THROUGH THE MEAN SQUARE ERROR (MSE) AND MEAN ABSOLUTE ERROR (MAE).

		Lin-RMM		Informer		LSTMa		ARIMA	
		MSE	MAE	MSE	MAE	MSE	MAE	MSE	MAE
ECL	48	<b>0.155</b>	<b>0.301</b>	0.239	0.359	0.493	0.539	0.879	0.764
	168	<b>0.175</b>	<b>0.322</b>	0.447	0.503	0.723	0.655	1.032	0.833
	336	<b>0.166</b>	<b>0.314</b>	0.489	0.528	1.212	0.898	1.136	0.876
	720	<b>0.164</b>	<b>0.314</b>	0.540	0.571	1.511	0.966	1.251	0.933
ETTh1	24	<b>0.029</b>	<b>0.127</b>	0.098	0.247	0.114	0.272	0.108	0.284
	48	<b>0.044</b>	<b>0.156</b>	0.158	0.319	0.193	0.358	0.175	0.424
	168	<b>0.079</b>	<b>0.211</b>	0.183	0.346	0.236	0.392	0.396	0.504
	336	<b>0.108</b>	<b>0.254</b>	0.222	0.387	0.590	0.698	0.468	0.593
ETTh2	24	<b>0.058</b>	<b>0.180</b>	0.093	0.240	0.155	0.307	3.554	0.445
	48	<b>0.083</b>	<b>0.220</b>	0.155	0.314	0.190	0.348	3.190	0.474
	168	<b>0.146</b>	<b>0.298</b>	0.232	0.389	0.385	0.514	2.800	0.595
	336	<b>0.186</b>	<b>0.347</b>	0.263	0.417	0.558	0.606	2.753	0.738
ETTh3	24	<b>0.275</b>	<b>0.427</b>	0.277	0.431	0.640	0.681	2.878	1.044
	48	<b>0.010</b>	<b>0.073</b>	0.030	0.137	0.121	0.233	0.090	0.206
	168	<b>0.018</b>	<b>0.098</b>	0.069	0.203	0.305	0.411	0.179	0.306
	336	<b>0.028</b>	<b>0.124</b>	0.194	0.372	0.287	0.420	0.272	0.399
ETTh4	288	<b>0.053</b>	<b>0.171</b>	0.401	0.554	0.524	0.584	0.462	0.558
	672	<b>0.079</b>	<b>0.209</b>	0.512	0.644	1.064	0.873	0.639	0.697
	24	<b>0.091</b>	<b>0.208</b>	0.117	0.251	0.131	0.254	0.219	0.355
	48	<b>0.135</b>	<b>0.260</b>	0.178	0.318	0.190	0.334	0.273	0.409
Weather	168	<b>0.222</b>	<b>0.345</b>	0.266	0.398	0.341	0.448	0.503	0.599
	336	<b>0.277</b>	<b>0.391</b>	0.297	0.416	0.456	0.554	0.728	0.730

TABLE III  
MULTIVARIATE PREDICTION PERFORMANCE OF THE STUDIED MODELS.

		Lin-RMM		f-Fedformer		w-Fedformer	
		MSE	MAE	MSE	MAE	MSE	MAE
ETTh2	96	<b>0.107</b>	<b>0.226</b>	0.203	0.287	0.204	0.288
	192	<b>0.140</b>	<b>0.263</b>	0.269	0.328	0.316	0.363
	336	<b>0.177</b>	<b>0.302</b>	0.325	0.366	0.359	0.387
	720	<b>0.223</b>	<b>0.349</b>	0.421	0.415	0.433	0.432
Exchange	96	0.874	0.680	0.148	0.278	<b>0.139</b>	<b>0.276</b>
	192	1.857	1.025	0.271	0.380	<b>0.256</b>	<b>0.369</b>
	336	2.819	1.306	0.460	0.500	<b>0.426</b>	<b>0.464</b>
	720	1.753	1.013	1.195	0.841	<b>1.090</b>	<b>0.800</b>
ILI	24	<b>1.549</b>	1.005	3.338	1.260	2.203	<b>0.963</b>
	36	<b>1.544</b>	1.003	2.678	1.080	2.272	<b>0.976</b>
	48	<b>1.279</b>	<b>0.885</b>	2.622	1.078	2.209	0.981
	60	<b>1.119</b>	<b>0.804</b>	2.857	1.157	2.545	1.061
Weather	96	2.677	0.876	<b>0.217</b>	<b>0.296</b>	0.227	0.304
	192	3.295	0.956	<b>0.276</b>	<b>0.336</b>	0.295	0.363
	336	2.926	0.939	<b>0.339</b>	<b>0.380</b>	0.381	0.416
	720	2.373	0.912	<b>0.403</b>	<b>0.428</b>	0.424	0.434

roughly similar, except for the ECL dataset where differences are large.

In general, Lin-RMM generally has a slightly better performance than both RC models. We interpret this as a confirmation that the versatility that Lin-RMM provides by learning how to combine the motifs translates in a small performance boost in prediction tasks. Indeed, this improvement appears to be sufficient enough to compensate for the detrimental effect of the lack of non-linearity.

## VI. DISCUSSION AND CONCLUSION

Motivated by the kernel view of reservoir models [23], we have introduced a simple, yet potentially surprisingly powerful model structure that decomposes the input signal along the time series motifs extracted from the reservoir kernel. This

idea seems to work for tested benchmark data very well even if the overall model structure is kept linear (linear readout).

Our model is transparent and amenable to analysis. Since the readout map is linear, one can study the magnitudes (absolute values) of the readout weights associated with different motif axis (columns of motif matrix  $\mathbf{M}$ ). As an example, we show in figures 1 and 2 the six most relevant motifs for the electricity consumption prediction (ECL dataset) associated with the 2 and 7 day prediction horizons, respectively. Interestingly (and intuitively enough), we can observe how the prediction model for the shorter prediction horizon (2 days) concentrates on higher frequency motifs than the model build for the longer 7-day horizon.

As another example, we we present in figures 3 and 4 six most relevant motifs for the electricity transformer oil

TABLE IV  
COMPARISON OF RESERVOIR MODELS WITH LIN-RMM.

		Lin-RMM		L-RC		NL-RC	
		MSE	MAE	MSE	MAE	MSE	MAE
ECL	48	<b>0.155</b>	<b>0.301</b>	0.228	0.369	0.341	0.451
	168	<b>0.175</b>	<b>0.322</b>	0.236	0.384	0.327	0.456
	336	<b>0.166</b>	<b>0.314</b>	0.242	0.388	0.341	0.469
	720	<b>0.164</b>	<b>0.314</b>	0.249	0.392	0.330	0.462
	960	<b>0.162</b>	<b>0.312</b>	0.249	0.393	0.321	0.455
ETTh1	24	<b>0.029</b>	<b>0.127</b>	0.032	0.135	0.031	0.128
	48	<b>0.044</b>	<b>0.156</b>	0.048	0.165	0.051	0.168
	168	<b>0.079</b>	<b>0.211</b>	0.091	0.226	0.109	0.249
	336	<b>0.108</b>	<b>0.254</b>	0.125	0.271	0.142	0.295
	720	<b>0.189</b>	<b>0.353</b>	0.198	0.360	0.219	0.386
ETTh2	24	<b>0.058</b>	0.180	0.072	0.199	0.058	<b>0.173</b>
	48	0.083	0.220	0.099	0.238	<b>0.082</b>	<b>0.212</b>
	168	0.146	0.298	0.164	0.313	<b>0.139</b>	<b>0.290</b>
	336	0.186	0.347	0.224	0.369	<b>0.185</b>	<b>0.337</b>
	720	0.275	0.427	0.315	0.450	<b>0.260</b>	<b>0.406</b>
ETTm1	24	<b>0.010</b>	<b>0.073</b>	0.012	0.078	0.011	0.074
	48	<b>0.018</b>	<b>0.098</b>	0.021	0.106	0.021	0.106
	96	<b>0.028</b>	<b>0.124</b>	0.031	0.131	0.037	0.140
	288	<b>0.053</b>	<b>0.171</b>	0.054	0.173	0.083	0.216
	672	0.079	0.209	<b>0.078</b>	<b>0.208</b>	0.138	0.282
Weather	24	<b>0.091</b>	<b>0.208</b>	0.108	0.232	0.093	0.209
	48	<b>0.135</b>	<b>0.260</b>	0.157	0.287	0.139	0.264
	168	<b>0.222</b>	<b>0.345</b>	0.259	0.380	0.223	0.353
	336	0.277	<b>0.391</b>	0.322	0.429	<b>0.271</b>	0.396

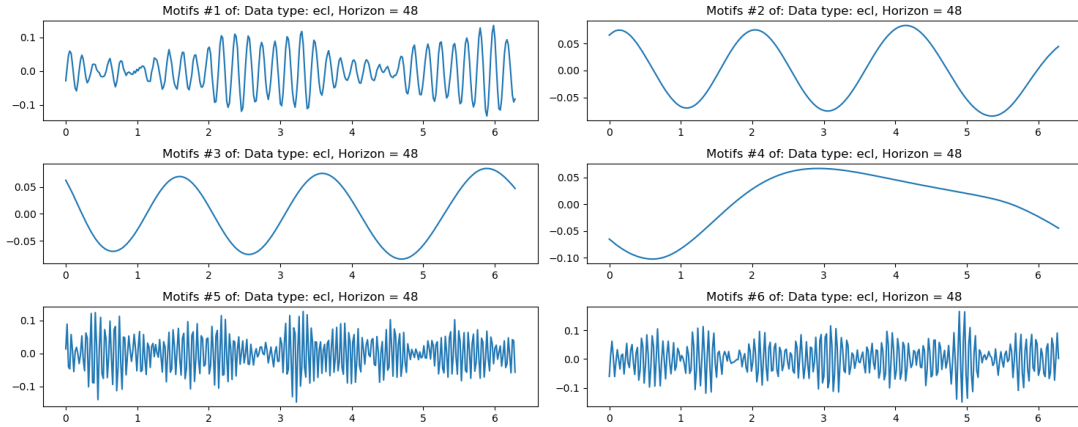


Fig. 1. Six most relevant motifs for the electricity consumption prediction (ECL dataset) - 48h (2 days) prediction horizon.

temperature prediction (ETTh dataset) employed by RMMs trained on 2-day prediction horizon task using data from two different regions in China. Note how a model for region 2 contains a very high frequency motif missing from the model specializing on region 1. Also a uni-modal "trend" motif for the region-1 model is replaced by the higher frequency bimodal one in the region-2 model. A deeper analysis of this form can help to unveil specific regional differences in the signal characteristics relevant for the prediction task with possible implications for the deployment strategy of electricity transformers

In general, our results demonstrate that simple models with easily controllable capacity that capture enough memory and subsequence structure can outperform (sometimes by a large

margin!) potentially over-complicated and over-parametrized deep learning models. Our conclusion is of course not that the reservoir motif based models are preferable to other potentially more complex alternatives, but rather that the temporal structure captured by the reservoir motifs generated from a reservoir model with just two free parameters can be sufficient for excellent predictive performance. Indeed, this echoes the message of [5].

We would suggest that when introducing new complex time series models one should always employ simple, but potentially powerful alternatives/baselines such as reservoir models or Lin-RMM introduced here.

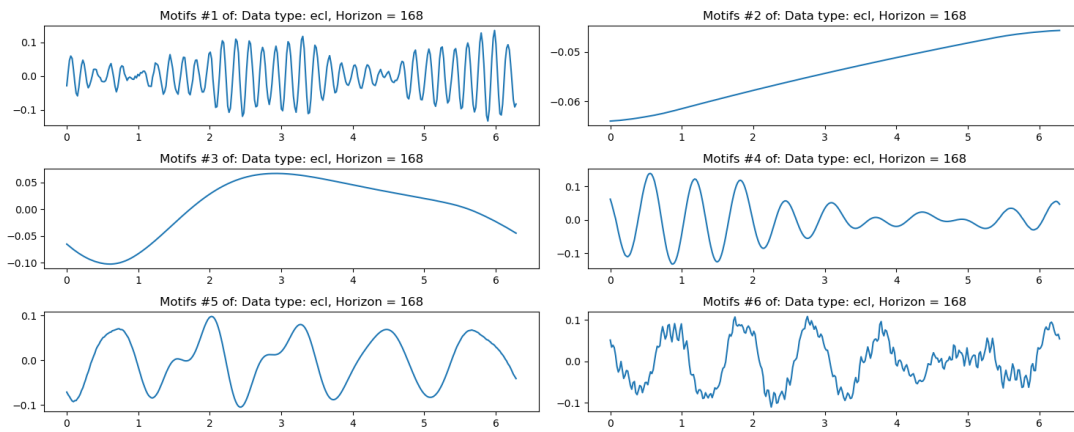


Fig. 2. Six most relevant motifs for the electricity consumption prediction (ECL dataset) - 168h (7 days) prediction horizon.

## REFERENCES

- [1] A. Vaswani, N. Shazeer, N. Parmar, J. Uszkoreit, L. Jones, A. N. Gomez, L. Kaiser, and I. Polosukhin, "Attention is all you need," 2023.
- [2] J. Devlin, M.-W. Chang, K. Lee, and K. Toutanova, "Bert: Pre-training of deep bidirectional transformers for language understanding," *arXiv preprint arXiv:1810.04805*, 2018.
- [3] H. Zhou, S. Zhang, J. Peng, S. Zhang, J. Li, H. Xiong, and W. Zhang, "Informer: Beyond efficient transformer for long sequence time-series forecasting," in *AAAI Conference on Artificial Intelligence*, 2020. [Online]. Available: <https://api.semanticscholar.org/CorpusID:229156802>
- [4] T. Zhou, Z. Ma, Q. Wen, X. Wang, L. Sun, and R. Jin, "Fedformer: Frequency enhanced decomposed transformer for long-term series forecasting," in *International Conference on Machine Learning*. PMLR, 2022, pp. 27 268–27 286.
- [5] A. Zeng, M. Chen, L. Zhang, and Q. Xu, "Are transformers effective for time series forecasting?" in *Proceedings of the AAAI conference on artificial intelligence*, vol. 37, no. 9, 2023, pp. 11 121–11 128.
- [6] R. E. Kalman, "Approach to linear filtering and prediction problems," *Journal of Basic Engineering*, vol. 82, no. 1, p. 35, 1960.
- [7] H. Jaeger, "The "echo state" approach to analysing and training recurrent neural networks," German National Research Center for Information Technology, Technical Report GMD report 148, 2001.
- [8] W. Maass, T. Natschlager, and H. Markram, "Real-time computing without stable states: a new framework for neural computation based on perturbations," *Neural Computation*, vol. 14(11), pp. 2531–2560, 2002.
- [9] P. Tino and G. Dorffner, "Predicting the future of discrete sequences from fractal representations of the past," *Machine Learning*, vol. 45(2), pp. 187–218, 2001.
- [10] M. Lukosevicius and H. Jaeger, "Reservoir computing approaches to recurrent neural network training," *Computer Science Review*, vol. 3(3), pp. 127–149, 2009.
- [11] H. Jaeger, "Short term memory in echo state networks," German National Research Center for Information Technology, Technical Report GMD report 152, 2002.
- [12] —, "A tutorial on training recurrent neural networks, covering bppt, rtl, ekf and the "echo state network" approach," German National Research Center for Information Technology, Technical Report GMD report 159, 2002.
- [13] H. Jaeger and H. Hass, "Harnessing nonlinearity: predicting chaotic systems and saving energy in wireless telecommunication," *Science*, vol. 304, pp. 78–80, 2004.
- [14] K. Bush and C. Anderson, "Modeling reward functions for incomplete state representations via echo state networks," in *Proceedings of the International Joint Conference on Neural Networks, Montreal, Quebec*, July 2005.
- [15] M. H. Tong, A. Bicket, E. Christiansen, and G. Cottrell, "Learning grammatical structure with echo state network," *Neural Networks*, vol. 20, pp. 424–432, 2007.
- [16] C. Gallicchio, A. Micheli, and L. Pedrelli, "Deep reservoir computing: A critical experimental analysis," *Neurocomputing*, vol. 268, pp. 87 – 99, 2017.
- [17] B. Schrauwen, M. Wardermann, D. Verstraeten, J. Steil, and D. Stroobandt, "Improving reservoirs using intrinsic plasticity," *Neurocomputing*, vol. 71(7-9), pp. 1159–1171, 2008.
- [18] J. Steil, "Online reservoir adaptation by intrinsic plasticity for backpropagation-decorrelation and echo state learning," *Neural Networks*, vol. 20, pp. 353–364, 2007.
- [19] Y. Xue, L. Yang, and S. Haykin, "Decoupled echo state networks with lateral inhibition," *Neural Networks*, vol. 20, pp. 365–376, 2007.
- [20] H. Jaeger, M. Lukosevicius, D. Popovici, and U. Siewert, "Optimisation and applications of echo state networks with leaky-integrator neurons," *Neural Networks*, vol. 20(3), pp. 335–352, 2007.
- [21] G. Holzmann and H. Hauser, "Echo state networks with filter neurons and a delay and sum readout," *Neural Networks*, vol. 32(2), pp. 244–256, 2009.
- [22] A. Gu, K. Goel, and C. Ré, "Efficiently modeling long sequences with structured state spaces," *arXiv preprint arXiv:2111.00396*, 2021.
- [23] P. Tino, "Dynamical systems as temporal feature spaces." *J. Mach. Learn. Res.*, vol. 21, pp. 44–1, 2020.
- [24] G. Lai, W.-C. Chang, Y. Yang, and H. Liu, "Modeling long-and short-term temporal patterns with deep neural networks," in *The 41st international ACM SIGIR conference on research & development in information retrieval*, 2018, pp. 95–104.
- [25] A. Rodan and P. Tino, "Minimum complexity echo state network," *IEEE transactions on neural networks*, vol. 22, no. 1, pp. 131–144, 2010.
- [26] B. Li, R. S. Fong, and P. Tiño, "Simple cycle reservoirs are universal," *arXiv preprint arXiv:2308.10793*, 2023.

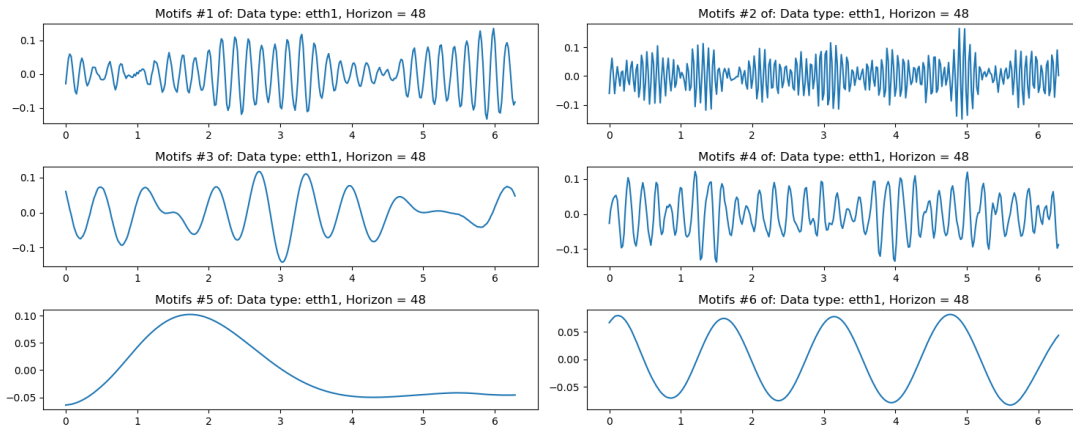


Fig. 3. Six most relevant motifs for the electricity transformer oil temperature prediction (ETTh dataset) - 48h (2 days) prediction horizon, region 1.

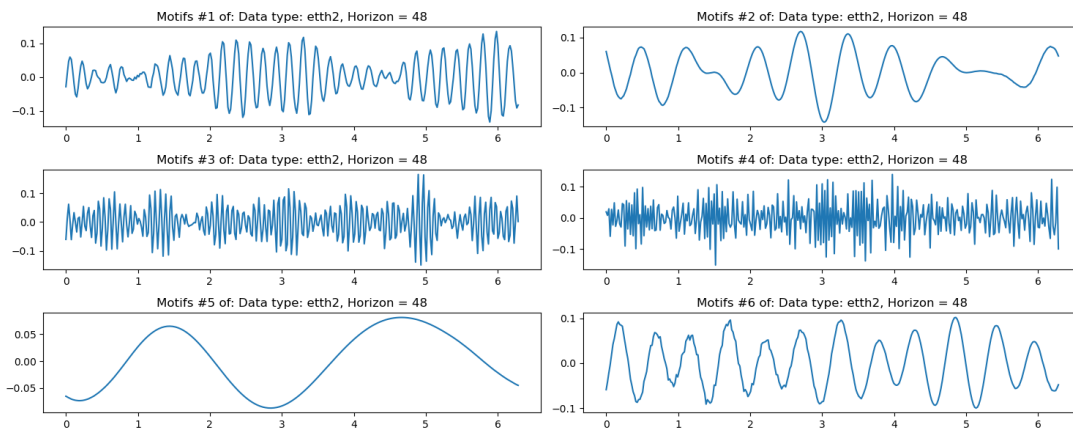


Fig. 4. Six most relevant motifs for the electricity transformer oil temperature prediction (ETTh dataset) - 48h (2 days) prediction horizon, region 2.